Acta Crystallographica Section D
Biological Crystallography
ISSN 0907-4449

Structure at 2.6 Å resolution of phenylalanyl-tRNA synthetase complexed with phenylalanyl-adenylate in the presence of manganese

Roman Fishman,[a] Valentina Ankilova,[b] Nina Moor[b] and Mark Safro[a]*

[a]Department of Structural Biology, Weizmann Institute of Science, Rehovot 76100, Israel, and [b]Novosibirsk Institute of Bioorganic Chemistry, Siberian Division of RAN, Novosibirsk 630090, Russia

Correspondence e-mail: mark.safro@weizmann.ac.il

Received 25 March 2001
Accepted 6 August 2001

PDB Reference: PheRS–Phe-AMP complex, 1jjc.

The crystal structure of phenylalanyl-tRNA synthetase (PheRS) from *Thermus thermophilus*, a class II aminoacyl-tRNA synthetase, complexed with phenylalanyl-adenylate (Phe-AMP) was determined at 2.6 Å resolution. Crystals of native PheRS were soaked in a solution containing phenylalanine and ATP in the presence of Mn^{2+} ions. The first step of the aminoacylation reaction proceeds within the crystals, resulting in Phe-AMP formation at the active site. Specific recognition of the phenylalanine portion of the Phe-AMP is achieved by interactions of the phenyl ring of Phe-AMP with two neighbouring residues, Pheα258 and Pheα260. No manganese ions were observed within the active site; their role in the formation of the transition state may be assigned to a number of polar residues and water molecules. In the anomalous Fourier difference map, a divalent metal ion was detected at the interface of the α- and β-subunits at a short distance from motif 3 residues participating in the substrate binding. A sulfate ion, which was identified on the protein surface, may mediate the interactions of PheRS with DNA. Visible conformational changes were detected in the active-site area adjacent to the position of the Phe-AMP, compared with the structure of PheRS complexed with a synthetic adenylate analogue (phenylalaninyl-adenylate). Based on the known structures of the substrate-free enzyme and its complexes with various ligands, a general scheme for the phenylalanylation mechanism is proposed.

1. Introduction

Aminoacyl-tRNA synthetases (aaRSs) comprise a family of enzymes that covalently attach amino acids to the corresponding nucleic acid adaptor molecules, tRNAs, prior to polypeptide-chain synthesis on ribosomes. Since protein synthesis depends on proper matching of an amino acid and its cognate tRNA, aaRSs substantially determine the overall specificity of protein synthesis. This is reflected in their own extreme specificity – only one mismatch reaction occurs for about 10^4–10^5 correctly paired amino acids and tRNAs (Yamane & Hopfield, 1977). Each enzyme is specific for only one amino acid and one or more cognate isoaccepting tRNAs (for reviews, see Delarue *et al.*, 1994; Arnez & Moras, 1997; Cusack, 1995). This covalent linkage is carried out through a two-step aminoacylation reaction. In the first step, the aaRS recognizes and binds the amino acid and ATP; the amino acid, activated by the enzyme, then attacks an α-phosphate of the ATP molecule, giving rise to a stable enzyme-bound intermediate molecule, aminoacyl-adenylate, and releasing inorganic pyrophosphate. Usually, this step requires divalent metal ions (Mg^{2+}) that stabilize the conformation of ATP and participate in the formation of adenylate. In the second step,

the amino-acid moiety is transferred to the 3′-terminal ribose of the cognate tRNA, generating the final product aminoacyl-tRNA and releasing AMP.

Despite the great diversity of aaRSs in amino-acid sequence and quaternary organization, comprehensive analysis of their sequences and three-dimensional structures led to the discovery of some common features and subsequently to the partitioning of the aaRSs family into two classes (Eriani *et al.*, 1990). The separation of aaRSs into two classes correlates not only with differences in the topologies of the catalytic domains but also with the stereochemical modes of attack on the carbonyl of the aminoacyl-adenylate. In this way, class I aaRSs attach amino acids to the 2′-OH group of the terminal ribose at the 3′-end of tRNA and class II enzymes attach the respective amino acids to the 3′-OH group of the terminal ribose. The only exception to this rule is phenylalanyl-tRNA synthetase (PheRS), although in accordance with the structural classification of class II enzymes, it attaches phenylalanine to the 2′-OH of the cognate $tRNA^{Phe}$.

At the present time, the structures of 18 of the 20 enzymes of the family, native or complexed with various substrates, intermediates and their analogues, are known. Nine of them belong to class II aaRSs: SerRS (Cusack *et al.*, 1990, 1996; Belrhali *et al.*, 1994, 1995; Biou *et al.*, 1994), GlyRS (Logan *et al.*, 1995; Arnez *et al.*, 1999), HisRS (Arnez *et al.*, 1995, 1997; Åberg *et al.*, 1997), ProRS (Cusack *et al.*, 1998), PheRS (Mosyak *et al.*, 1995; Goldgur *et al.*, 1997; Reshetnikova *et al.*, 1999), AsnRS (Berthet-Colominas *et al.*, 1998), LysRS (Onesti *et al.*, 1995; Cusack *et al.*, 1996; Desogus *et al.*, 2000), AspRS (Ruff *et al.*, 1991; Cavarelli *et al.*, 1994; Delarue *et al.*, 1994; Poterszman *et al.*, 1994; Schmitt *et al.*, 1998) and ThrRS (Sankaranarayanan *et al.*, 1999).

The most complex representative of the aaRS family, *T. thermophilus* PheRS, possesses a heterodimeric subunit organization $(\alpha\beta)_2$ with a molecular mass of ∼252 kDa (350 amino acids in the α-subunit and 785 in the β-subunit; Mosyak *et al.*, 1995). Neither the α nor β monomers nor the α_2, β_2 or $\alpha\beta$ dimers manifest catalytic activity in aminoacylation and aminoacyl-adenylate formation (Khodyreva *et al.*, 1985; Bobkova *et al.*, 1991). PheRS is structurally and functionally an $(\alpha\beta)_2$ heterodimer (Mosyak *et al.*, 1995); nevertheless, the β-subunit is not directly involved in the aminoacylation reaction.

The structure of PheRS complexed with $tRNA^{Phe}$ (Goldgur *et al.*, 1997) makes it apparent that the major function of the β-subunit is the recognition and binding of $tRNA^{Phe}$. The entire $(\alpha\beta)_2$ molecule interacts with two $tRNA^{Phe}$ molecules. The structure of the complex revealed true cross-subunit tRNA binding: one $tRNA^{Phe}$ interacts with all four subunits of the enzyme. The CCA end and the acceptor stem of the $tRNA^{Phe}$ molecule interact with the active site located in the α-subunit and with the B1 domain of the same heterodimer, while the anticodon loop of the $tRNA^{Phe}$ is specifically recognized by the C-terminal domain of the β*-subunit (or B8*, where * indicates the second heterodimer). 85 residues at the N-terminus of the α-subunit form a helical arm built up of two long antiparallel α-helices which stretch out into solvent by 65 Å. This region is apparently flexible in the absence of contacts with tRNA and appears disordered in the electron-density map of native PheRS. The helical arm of the α*-subunit approaches the tRNA mainly from the variable-loop side. Thus, the structures of the native enzyme and its complex with $tRNA^{Phe}$ account for the enzyme being a functional $(\alpha\beta)_2$ dimer.

The active site of PheRS is generated by a catalytic module (CAM) only and comprises residues 102–327 of the α-subunit (Mosyak *et al.*, 1995). The three conserved motifs characteristic of class II aaRSs are located in the CAM: motif 1 (residues 102–125), motif 2 (residues 199–220) and motif 3 (312–327). The latter two provide the functional basis of the active site.

In our previous paper describing the structure of the PheRS–$tRNA^{Phe}$ complex (Goldgur *et al.*, 1997), the suggestion was made that variations in the position of the 3′-terminal adenosine of $tRNA^{Phe}$ may be the only factor causing the difference between PheRS and other representatives of class II aaRSs in the characteristic primary site of aminoacylation. Recently determined crystal structures of *T. thermophilus* PheRS complexed with phenylalanine and a synthetic adenylate analogue (PheOH-AMP) have further elucidated the class- and system-specific net of interactions, stabilizing the positions of the amino-acid, adenine and sugar moiety of the analogue (Reshetnikova *et al.*, 1999). Our findings (see below) together with these data imply that the peculiarity of the aminoacylation site in the phenylalanine system is governed by stepwise (ordered) fine adjustments of all the reactants and their intermediates in the active sites.

The structures of AspRS and SerRS complexed with ATP, aminoacyl-adenylate or aminoacyl-adenylate analogues showed the presence of magnesium ions in the active-site areas. The availability of the Mg^{2+} ions or other divalent ions should presumably stabilize the bent ATP conformation and was postulated as the conceptually necessary condition for transition-state formation in the majority of class II systems. PheRS from *T. thermophilus* as well as its complexes with ligands have been crystallized (Chernaya *et al.*, 1987) from solution containing ∼28% saturated ammonium sulfate (AS). As previously reported (Belrhali *et al.*, 1995), this or similar crystallization media may prevent the binding of magnesium ions at proper positions in the active site. This was probably the reason why phenylalanyl-adenylate could not be observed in the active site of PheRS (Reshetnikova *et al.*, 1999) when the crystals had been soaked in a solution containing phenylalanine, ATP and Mg^{2+}. However, if in the original AS-containing reaction mixture (Chernaya *et al.*, 1987) manganese ions are substituted for the magnesium, a new assay demonstrates reasonable aminoacylation activity (see below), thus implying phenylalanine activation at the first step of the aminoacylation reaction.

In order to elucidate all the interactions of the system intermediate (phenylalanyl-adenylate) with residues exposed to the active-site area, to localize the positions of possible divalent metal ions in PheRS and to follow the course of the system-specific mechanism of aminoacylation, the crystal

Table 1
Data-collection and model-refinement statistics.

	PheRS native	PheRS–Phe-AMP
Data collection		
Space group	$P3_221$	$P3_221$
Unit-cell parameters (Å)	$a = b = 173.3$, $c = 138.4$	$a = b = 173.6$, $c = 138.3$
Resolution (Å)	50.0–2.8	50.0–2.6
R_{merge}† (%)	7.2	7.9
Redundancy (%)	5.2	5.3
Completeness total (last shell) (%)	97.6 (72.2)	94.7 (81.7)
Total reflections	307582	405589
Unique reflections	59314	75189
Structure refinement		
No. of atoms	8250	8284
No. of water molecules		289
Ions	Mn^{2+}	Mn^{2+}, SO_4^{2-}
R factor‡ (%)		21.6
R_{free} (%)		25.8
Average B factor (Å^2)		45.2
R.m.s. bonds (Å)		0.011
R.m.s angles (°)		1.76

† $R_{merge} = \sum_{hkl}\sum_j |I_j(hkl) - \langle I_j(hkl)\rangle|/\sum_{hkl}\sum_j I(hkl)$, where $I_j(hkl)$ and $\langle I_j(hkl)\rangle$ are the intensity of measurement j and mean intensity for the reflection with indices hkl, respectively. ‡ R factor $= \sum(F_{obs} - kF_{calc})/\sum_{hkl} F_{obs}$, where k is a scale factor and R_{free} is the R factor for the test set of reflections not used during refinement (10% of the data set).

structure of PheRS complexed with the true intermediate phenylalanyl-adenylate (synthesized within the native PheRS crystals soaked with phenylalanine, ATP and $MnSO_4$) has now been determined at 2.6 Å.

2. Materials and methods

2.1. Crystal preparation and data collection

Native PheRS was extracted from *T. thermophilus* HB8 and purified as described previously (Chernaya *et al.*, 1987). Prior to crystallization, the protein was dialyzed overnight against crystallization buffer (20 m*M* imidazole–HCl pH 7.8, 1 m*M* $MgCl_2$, 1 m*M* NaN_3). The protein was collected and precipitated for 8 h at 277 K in 53% saturated AS. It was then centrifuged for 45 min (12 000 rev min^{-1}, 277 K). Supernatant was removed and the pellet was resuspended in crystallization buffer and dialyzed overnight against a crystallization buffer containing 10% AS. The protein solution was then centrifuged for 5 min (6000 rev min^{-1}, 277 K) to remove small particles and dust.

Native crystals were grown by the 'hanging-drop' method using AS as a precipitating agent (crystallization buffer containing 27% saturated AS). Crystals grew to maximum dimensions of 0.4 × 0.4 × 0.3 mm.

To obtain a complex of the protein with the product of the first step of the aminoacylation reaction (phenylalanyl-adenylate, Phe-AMP), apoenzyme crystals were soaked for 48 h in a solution containing 20 m*M* imidazole–HCl pH 7.8, 2.5 m*M* ATP, 2.5 m*M* L-phenylalanine, 1 m*M* NaN_3, 38% $(NH_4)_2SO_4$ and 6.0 m*M* $MnSO_4$.

Two data sets were collected at the NSLS in Brookhaven at a wavelength of 0.98 Å and a crystal-to-detector distance of 120 mm. A single flash-frozen crystal at a temperature of 100 ± 0.2 K was used for each experiment. The Brandeis CCD-based detector on beamline X12C was employed for data collection. Before flash-cooling, the crystals were transferred into a cryoprotective solution containing 30%(*v*/*v*) glycerol. The first data set was collected for native crystals at 2.8 Å resolution. A total of 60 frames were collected from a single crystal with an oscillation range of 1° and an exposure time of 120 s frame^{-1}. The second data set (60 frames) was collected from soaked crystals at 2.6 Å resolution with the same exposure time and oscillation range.

Data were processed with the *HKL* package (Otwinowski, 1993) and scaled with the *CCP*4 suite (Collaborative Computational Project, Number 4, 1994). Data-collection statistics are summarized in Table 1.

2.2. Model building and refinement

The 2.9 Å refined model of *T. thermophilus* PheRS (Mosyak *et al.*, 1995) was used as a starting model. This model was first subjected to rigid-body refinement using a 20–2.8 Å data set collected from the native crystals at 100 K. The refinement procedures were carried out using the program *CNS* (Brunger *et al.*, 1998). The initial R factor of 44.3% was reduced to 34.4% by rigid-body refinement. Several rounds of Cartesian coordinate energy minimization, simulated annealing and manual revision of the model using the program *O* (Jones *et al.*, 1991) resulted in a rapid decrease in the R and R_{free} values to 26.5 and 31.0%, respectively. A random sample containing 10% of the reflections in the data set was excluded from the refinement and used for R_{free} calculation. Additional refinement of group B factors followed by energy minimization lowered the R and R_{free} values to 23.9 and 29.2%, respectively. The resulting model of apo PheRS was used for difference Fourier map calculation and as a preliminary model of the structure of the complex.

The initial electron-density map with coefficients $F_{obs} - F_{calc}$ and $2F_{obs} - F_{calc}$ was built using *SIGMAA* (Read, 1986). These and all subsequent calculations were performed against the F_{obs} data set at 50–2.6 Å resolution for the Phe-AMP complex. The map showed well defined electron density for the ligand at the active site and a very high (over 10σ) peak for an Mn^{2+} ion bound at the α/β-subunit interface. The Phe-AMP model was built into the difference density and manually adjusted with the program *O* (Jones *et al.*, 1991). The initial R and R_{free} values of the PheRS–Phe-AMP complex in the presence of Mn^{2+} were estimated as 30.1 and 31.7%, respectively. After a round of refinement alternating with model refitting into the maps, R and R_{free} decreased to 23.8 and 27.0%, respectively. Water molecules located within hydrogen-bonding distance of the PheRS–Phe-AMP complex and associated with electron density peaks >3.0σ were added and resulted in 290 molecules. Addition of water to the complex model was followed by individual B-factor refinement.

For positioning metal ions within the protein model, an anomalous difference map was calculated with coefficients

$(\Delta F_{ano})_{Mn} \exp[i(\varphi_c^{nat} - \pi/2)]$. An anomalous map should allow unambiguous location of the manganese ion present in the structure (Pepinsky & Okaya, 1956). This map demonstrated one high (>8σ) and clear peak for the cation bound at the α/β-subunit interface in the vicinity of the active centre. No anomalous signal was detected inside the active centre itself.

The model refinement of the complex finally converged to an R value of 21.6% and R_{free} of 25.8% with good stereochemistry. The refined structure was analyzed using the program *PROCHECK* (Laskowski *et al.*, 1993). The analysis showed that all but one of the non-glycine ψ and φ values lie in the allowed regions of the Ramachandran plot, with 88.4% in the most favourable regions. Residue Gluβ579, which is located in the generously allowed region, is involved in a three-residue γ-turn (Richardson, 1981). The final model contains 8249 non-H protein atoms, 34 non-H atoms of Phe-AMP, 289 water molecules, one SO_4^{2-} ion and one Mn^{2+} ion. Final refinement statistics are presented in Table 1.

3. Results and discussion

3.1. The aminoacylation reaction in the presence of divalent ions

The aminoacylation reaction does not proceed when sulfate and magnesium ions are concurrently present in the reaction mixture (see above). However, aminoacylation can occur even at relatively high AS concentration if magnesium ions are replaced by manganese. In both SerRS and HisRS, manganese can bind in the active sites and interact with ATP even at a 40% saturation of AS. If the AS-containing mother liquor was substituted within the crystals (Belrhali *et al.*, 1995) by 56% saturated sodium citrate, Ser-AMP was formed in the presence of Mg^{2+} and observed in the electron-density map. These data indicate that sulfate ions interfere with magnesium binding in the active site and cannot be displaced from the active site by the substrates, thereby inhibiting the aminoacylation reaction for at least several aaRSs. To ensure that Mn^{2+} ions may substitute for Mg^{2+} when charging the cognate tRNA molecules in the phenylalanine system, the activity of PheRS from *T. thermophilus* was assayed (Ankilova *et al.*, 1988) by aminoacylation of the total *Escherichia coli* $tRNA^{Phe}$ (an efficient heterologous substrate of the thermophilic PheRS) with L-[^{14}C]-phenylalanine in the presence of ATP and manganese (alternatively, in the reaction mixture Mn^{2+} was replaced by Mg^{2+}) ions. The results presented in Fig. 1 demonstrate that the enzyme can transfer and therefore activate phenylalanine in the presence of Mn^{2+} ions. Nevertheless, the lesser effectiveness of these ions in the formation of the intermediate products can keep the sulfates out of the crucial positions.

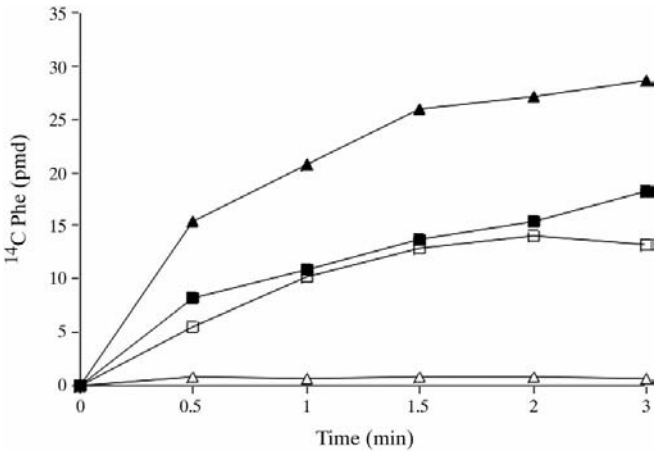

Figure 1
Rates of aminoacylation of total *E. coli* $tRNA^{Phe}$ catalyzed by *T. thermophilus* PheRS, in accordance with the nature of metal ion and the availability of the ammonium sulfate in reaction mixture. The reaction was carried out at 298 K as described in Ankilova *et al.* (1988). Filled triangles, 9 m*M* $MgCl_2$; empty triangles, 9 m*M* $MgCl_2$, 35% saturated AS; filled squares, 8 m*M* $MnCl_2$; empty squares, 8 m*M* $MnCl_2$, 35% saturated AS.

3.2. The overview of the PheRS complexed with Phe-AMP

The crystal structure of PheRS complexed with the product of the first step of the aminoacylation reaction, Phe-AMP, was solved at 2.6 Å resolution. A difference Fourier map with amplitudes and phases based on the refined native model made it apparent that there is strong extra positive density which could be attributed to the entire Phe-AMP molecule in the active site (Fig. 2). This result shows that the PheRS is active in the crystal for the formation of Phe-AMP in the presence of manganese.

The N-terminal region of the α-subunit (domain A0, residues 1–85), which comprises a coiled-coil structure upon tRNA binding (Goldgur *et al.*, 1997), did not show up at the flash-freezing temperature (100 K) and remained disordered, as observed in the electron-density map of the apoenzyme at room temperature (Mosyak *et al.*, 1995). These residues were not included in the model. Curiously, it was found that the average B factor of the PheRS–Phe-AMP complex is ~45 Å^2, compared with the value of ~69 Å^2 obtained for the PheRS–Phe complex (Reshetnikova *et al.*, 1999). Most of the atoms with high B values are located in the B8 domain of the β-subunit, especially at its C-terminus, or belong to the flexible loops of the β-subunit (loops 97–102, 599–602 and 676–691). This might be the reason why we could trace the C-terminus of the β-subunit (anticodon-binding domain, B8) unambiguously. The side chains of six C-terminal residues with atomic B factors >95 Å^2 are not visible in the electron-density map. From comparison of the PheRS–Phe-AMP complex with that of the synthetic adenylate analogue (Reshetnikova *et al.*, 1999) it is apparent that for 1041 equivalent C^α atoms the r.m.s. deviation is 0.63 Å (for all the atoms included in the heterodimer $\alpha\beta$, this value is 1.2 Å).

Superposition of the C^α trace of the apo enzyme on those of the PheRS–Phe-AMP complex displays a maximal conformational shift (~3.5 Å) in the 97–102 loop region of the β-subunit. This flexible loop is far from the active site, which is located in the α-subunit. The substrate binding should not have a pronounced effect on the structural rearrangements in this area. At the same time, the main-chain and side-chain atoms in this loop have rather high atomic B factors

(~85–90 Å^2). It is possible that the concerted displacement of the loop may indicate some electron density corresponding to an alternative conformation. In the Phe-AMP-bound structure there are residues in the vicinity of the active site whose side chains have swung a considerable distance towards the substrate from their original positions in the apoenzyme (see below).

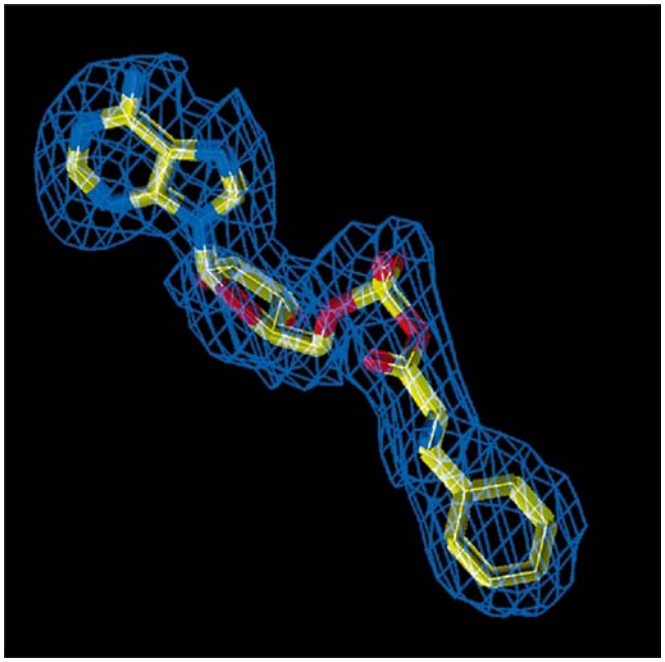

Figure 2
A part of the final $2F_{obs} - F_{calc}$ electron-density map showing electron density for Phe-AMP. A map was calculated using all data from 50 to 2.6 Å resolution from a model of the PheRS–Phe-AMP complex contoured at 1.0σ.

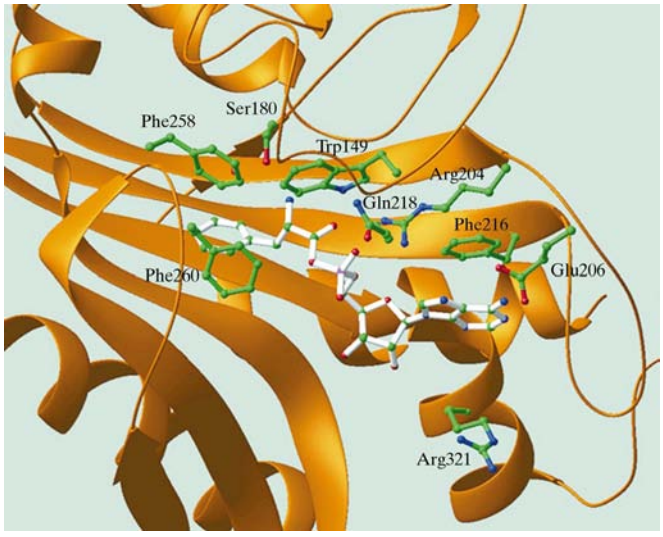

Figure 3
Ribbon representation (Carson, 1997) showing the principal interactions between phenylalanyl-adenylate and PheRS. Phe-AMP and side chains of the key residues in the active site are drawn in ball-and-stick representation. Amino-acid residues of the enzyme are coloured green, while the substrate is white.

As already mentioned, in addition to 8249 non-H atoms in the $\alpha\beta$ heterodimer, 290 water molecules were picked in the model. Of the solvent molecules, one has an extremely low B factor (3 Å^2) and it is notable that this atom has been identified with a strong peak of electron density on the $2F_o - F_c$ map (~7σ) and is located on the surface of the B5 domain, near the intramolecular twofold-symmetry axis. The position of the atom is coordinated by two arginines, Argβ407 and Argβ413. The large size of the peak (a few ångströms in diameter), its almost spherical shape and the geometry of its interaction with the guanidinium groups of the arginines suggest that this solvent molecule might be a sulfate ion (as described below).

3.3. Phenylalanyl-adenylate binding and recognition

The active-site area on the α-subunit is formed mainly by six antiparallel strands and one parallel strand organized in a β-sheet interconnected with α-helices and loops (Fig. 3). Its topology is common for class II synthetases and involves highly conserved residues from motifs 2 (residues 199–220) and 3 (residues 312–327). All conformational changes at the active site that were observed upon phenylalanyl-adenylate complex formation have the effect of a general shift towards the area where the Phe-AMP molecule is bound. In particular, the constituent loop of motif 2 is slightly shifted by 1.1 Å towards the adenine moiety. In the apoenzyme, as well as in the complex structure, the conformation of the motif 2 loop is

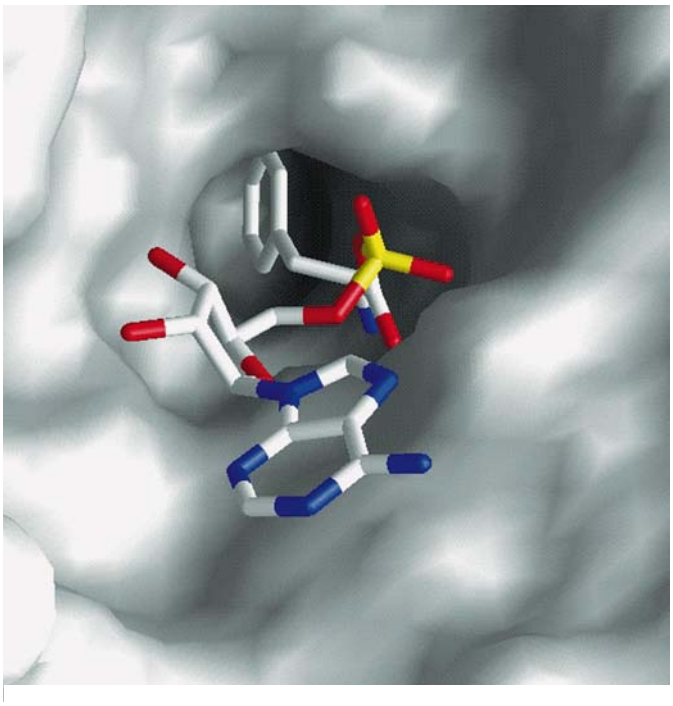

Figure 4
Protein surface in the active-site region of PheRS and its complementarity with the bound phenylalanyl-adenylate using the *GRASP* program (Nicholls *et al.*, 1991). The phenylalanyl-adenylate is represented as a stick model. The amino-acid moiety deeply penetrates into a cavity on the protein surface.

well defined and portions of the electron density corresponding to the side chains of all residues are well ordered.

A distinctive feature of the topology of the PheRS active site is the presence of a deep phenylalanine-binding pocket (Fig. 4). The bottom surface of the pocket is parallel to the phenyl ring of the substrate and is covered by the invariant glycines (282, 284, 312, 316 and 318), thus providing the space required for the phenylalanine and ATP moieties. One of the walls and the top surface of the pocket are covered by hydrophobic residues only: Pheα258, Pheα260, Valα261 and Ileα139. Another wall of the pocket is made up entirely of residues which may participate in electrostatic interactions and in the formation of hydrogen bonds: Gluα220, Serα180, Hisα178 and Glnα218. Such an anisotropy in the distribution of hydrophobic and hydrophilic residues within the pocket unambiguously indicates the orientation of the amino and carbonyl groups of the amino-acid moiety of Phe-AMP.

Specific recognition of the phenylalanine is achieved by interactions wherein the substrate phenyl ring and two neighbouring phenyl rings of Pheα258 and Pheα260 from motif 3 make a 'network' of interactions; each aromatic pair is arranged with 'edge-to-face' contacts, as shown in Fig. 5. The appearance of the phenylalanine substrate in such an environment makes the attractive potential energy of interaction twice as large as a single 'edge-to-face' aromatic–aromatic interaction and thus makes the Phe/PheRS recognition highly specific and very favourable energetically. The ligand phenyl ring centroid is separated from the Pheα258 centroid by 4.6 Å. The distance between the centroids of Pheα260 and Phe-AMP is 5.2 Å and that between the Pheα258/Pheα260 pair is 5.9 Å. These values are consistent with the observation deduced from a large number of protein structures that phenyl ring centroids are commonly separated by about 5.5 Å (Burley & Petsko, 1985). The dihedral angles within this 'network' approach 90°, which also corresponds to the most commonly encountered values. It is interesting to note that the active site of PheRS itself contains a stretched 'network' of aromatic–aromatic interactions that successively include Pheα258→Pheα260→Trpα149→Pheα134 and Trpα153.

The anchoring of the amino group of the substrate is achieved by its interactions with Serα180, Hisα178 and with the well ordered water molecule S9. The amino group of phenylalanine forms water-mediated interactions through the S9 molecule with Gluα220, Glnα218 and Thrα179 (Fig. 6 and Table 2). It is interesting to note the concerted conformational switch of Gluα220 and Glnα218 compared with the native structure. Under this realignment, the S9 water molecule occupies a highly coordinated position in the vicinity of the Phe-AMP and the new position of Glnα218 favours its hydrogen bonding with O4′ and O5′ of the ribose in addition to the carbonyl O atom of the amino acid. Multiple sequence alignment between PheRSs from different prokaryotic and eukaryotic sources (Rodova *et al.*, 1999) shows that residues Glnα218 and Gluα220 are strictly conserved in all referenced sequences. For the two residues Thrα179 and Serα180, conservation can be assigned to the hydroxyl group which occurs in these residues. Amino acids Ser and Thr substitute for one another at positions 179 and 180. Hisα178 is in some cases replaced by glutamine, which is uncharged but has a polar amide group with extensive hydrogen-bonding capacity.

PheRS complexed with Phe-AMP, as noted above, reveals less dramatic conformational changes in motif 2 relative to the apo enzyme compared with SerRS from *T. thermophilus* and yeast AspRS. In fact, a whole region of electron density adjacent to the Phe-AMP, including the side chain of Argα204, is well ordered in both the native and complex structures. The fully extended conformation of Argα204, clearly visible on the map, makes possible simultaneous contacts of its side chain with the α-phosphate and carbonyl O atom of the substrate. When compared with native PheRS, it looks as if the side chain has been pulled out towards the substrate from its original conformation. On the opposite side of the substrate (opposite to the bond Argα204—phosphate), water molecule S290 bridges the phosphate O atom with the main-chain carbonyl O atom of Metα148, significantly strengthening the interaction of the

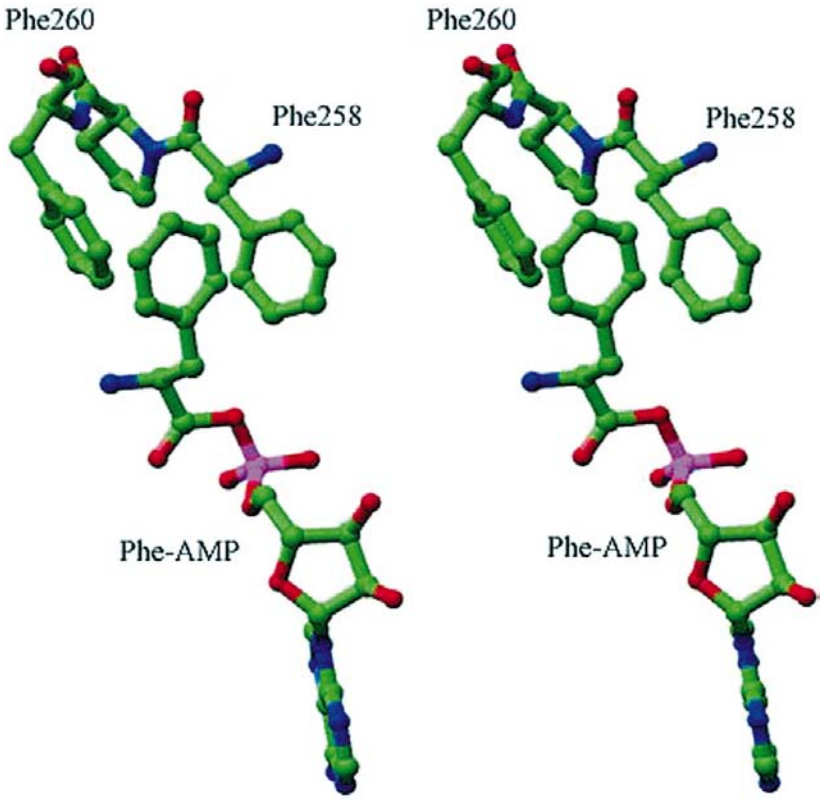

Figure 5
Stereoview of the three aromatic rings that form triple 'edge-to-face' aromatic interactions at the active site of PheRS: the phenyl ring of phenylalanyl-adenylate interacts with Pheα258 and Pheα260 from the highly conserved synthetase motif 3.

aminoacyl-adenylate with the enzyme. Thus, the two regions of the active site are tied together by interactions of the phosphate and ribose with Argα204 and Glnα218 on one side and with the carbonyl O atom of Metα148 (*via* water molecule S290) on the other.

The ribose moiety is held in position by Glnα218 and water molecule S208, which is hydrogen bonded to 2′-OH and the NH_2 group of Argα321. The water molecule S154 bridges 3′-OH of the ribose and the side chain of the fully conserved Gluα279. Here, we emphasize that there is no direct interaction between Gluα279 and the 3′-hydroxyl group: the carboxylic group of the Gluα279 side chain swings aside 90° from the ribose moiety and participates in tetracoordination of water molecule S195 together with Argα252, Glnα254 and Glnα266. Among class II aaRSs, PheRS is not exceptional in that respect: in HisRS from *E. coli* glutamic acid in this position is replaced by alanine, which lacks the ability for hydrogen bonding and thus 3′-OH of histidyl-adenylate is free of direct interactions with the enzyme (Arnez *et al.*, 1995). A different situation emerges for AspRS, SerRS and LysRS, where highly conserved glutamic acid residues interact directly with 3′-OH of the ribose. Moreover, a repulsive electronegative environment created by topologically equivalent triads of glutamic acids in each of the above-mentioned synthetases (for AspRS, Asp475, Glu482 and Asp282; for SerRS, Asp332, Glu345 and Glu334; for LysRS, Glu414, Glu421 and Glu380) prevents reorientation of the referred glutamic acids away from the ribose in the active site to the protein surface as occurs in PheRS. Thus, the conformational constraints of the adenylate ribose appear to be dictated exclusively by a local system-specific net of hydrogen bonds and are not necessarily retained in class II or in their associated subclasses.

The binding mode of the adenosine portion of phenylalanyl-adenylate has much in common with those observed for other class II aaRSs complexes and is predominantly associated with Pheα216 and Argα321, which clamp adenine between the phenyl ring of Pheα216 and the aliphatic portion of the Argα321 side chain. These residues are strictly conserved within class II aaRSs and are positioned in motifs 2 and 3, respectively. Upon formation of the PheRS–Phe-AMP complex, the side chain of Argα321 undergoes large conformational changes, as revealed in the electron-density map. It switches to interact with the adenine ring and the observed movement is larger than 4.5 Å for the CZ atom. However, the reoriented guanidinium group is not coplanar with the adenine ring. The well ordered portion of the electron density associated with it is directed outward from the adenine ring. The adenine moiety is additionally anchored through hydrogen bonding between N6 and N1 of the adenine ring with Gluα206 and the main-chain atoms of Gluα213 (carbonyl and amide groups). It is notable that the position occupied by loop 205–214 and the conformation of Gluα213 side chain provide the phenylalanine system with a strengthened network of hydrogen bonding between N6 and two O atoms of Gluα206 compared with other class II aaRSs. Two water molecules complete the net of interactions that stabilize the orientation of the adenine in the active site. Water molecule S208 bridges the main-chain carbonyl O atom of Glyα318, the amide N atom of Argα321, the ribose 2′-hydroxyl group and N3 of adenine, completing the tetracoordination. The guanidinium group of class II invariant Argα204 is bound to the N7 of adenine *via* water molecule S289.

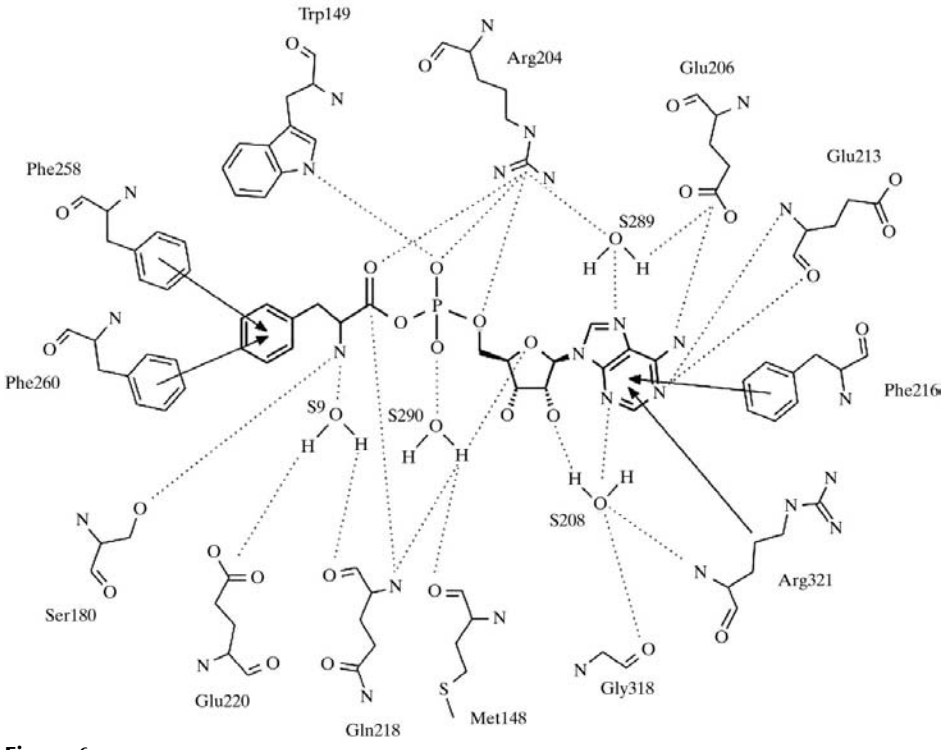

Figure 6
Schematic representation of the principal interactions between PheRS and phenylalanyl-adenylate at the active site. Hydrogen bonds are shown by dashed lines and van der Waals interactions by solid arrows.

3.4. The structural basis of the phenylalanine discrimination among the aromatic amino acids

Of the 20 amino acids, there are only three residues with bulky aromatic side chains which might be considered as candidates for specific binding in the active site of PheRS, since the phenylalanine-recognition process is essentially driven by a 'network' of aromatic–aromatic interactions (see above). In fact, the scheme of van der Waals contacts in the interior of the phenylalanine-binding pocket (Fig. 7) shows clearly why Trp and Tyr cannot be correctly positioned at this site so as to react

Table 2
The list of major interactions between atoms of phenylalanyl-adenylate and PheRS.

Phenylalanyl-adenylate	Type of interaction†	Protein residue	Interacting atom/group	Distance (Å)
Amino-acid side chain				
Phenyl ring	AA	Pheα258	Phenyl ring	4.6
Phenyl ring	AA	Pheα260	Phenyl ring	5.2
Phenyl ring	Stacking	Alaα314 (3)	C^{β}	4.1
Phenyl ring	Stacking	Pheα315 (3)	C^{α}	3.6
Phenyl ring	Stacking	Glyα316 (3)	C^{α}	3.7
Phenyl ring	Stacking	Valα261	$C^{\gamma 1}$	4.0
Phenyl ring	Stacking	Valα261	$C^{\gamma 2}$	4.2
Phenyl ring	Stacking	Alaα283	C^{α}	3.5
Phenyl ring	Stacking	Glyα282	C^{α}	3.8
Amino-acid main chain				
NH_2	HB	Hisα178	$N^{\delta 1}$	2.8
NH_2	HB through S9	Thrα179	$O^{\gamma 1}$	3.1 and 3.0
NH_2	HB	Serα180	O^{γ}	2.8
NH_2	HB through S9	Glnα218 (2)	$O^{\varepsilon 1}$	3.1 and 2.7
NH_2	HB through S9	Gluα220 (2)	$O^{\varepsilon 1}$	3.1 and 3.2
O	HB	Trpα149	$N^{\varepsilon 1}$	3.4
O	HB	Argα204 (2)	$N^{\eta 1}$	2.8
O	HB	Glnα218 (2)	$N^{\varepsilon 2}$	3.0
Phosphate				
O1P	HB	Argα204 (2)	$N^{\eta 1}$	2.7
O1P	HB	Argα204 (2)	$N^{\eta 2}$	2.6
O1P	HB through S290	Metα148	$N^{\varepsilon 1}$	3.3
OP2	HB through S290	Metα148	O	3.1 and 3.3
Ribose				
O2′	HB through S208	Glyα318 (3)	O	3.1 and 3.3
O2′	HB through S208	Argα321 (3)	N	3.1 and 3.4
O3′	HB through S154	Gluα279	$O^{\varepsilon 1}$	3.5 and 3.5
O3′	HB	Glyα281	O	2.9
O4′	HB	Glnα218 (2)	$N^{\varepsilon 2}$	3.4
O5′	HB	Glnα218 (2)	$N^{\varepsilon 2}$	3.0
Adenine				
Adenine ring	AA stacking	Pheα216 (2)	Phenyl ring	~2.8
Adenine ring	Stacking	Argα321 (3)	Side chain	~5.2
N1	HB	Gluα213 (2)	N	3.2
N3	HB through S208	Glyα318 (3)	O	2.9 and 3.0
N3	HB through S208	Argα321 (3)	N	2.9 and 3.3
N6	HB	Gluα206 (2)	$O^{\varepsilon 1}$	3.3
N6	HB	Gluα206 (2)	$O^{\varepsilon 2}$	3.3
N7	HB through S289	Argα204 (2)	$N^{\eta 1}$	2.8 and 3.3

† HB stands for hydrogen bond; 'HB through S289' implies that two atoms (N7 and $N^{\eta 1}$) interact through water molecule S289; thus, '2.8 and 3.3' indicates that the distance between the N7 atom of the adenine ring and water molecule S289 is 2.8 Å and the distance between S289 and the $N^{\eta 1}$ atom of Arg204 is 3.3 Å *etc.*; 'AA' implies aromatic–aromatic interactions.

with ATP and form aminoacyl-adenylate. Taking into account a predetermined net of interactions with the α-amino group and carbonyl O atom of the amino acid, it is not feasible to insert the bulky side chain of Trp without a serious rearrangement of the active-site conformation. Thus, the only amino acid remaining is tyrosine, which differs from phenylalanine by an additional OH group attached to the phenyl ring. As shown by Fig. 7, both steric hindrance and the hydrophobic nature of the back wall of the amino-acid binding pocket (Valα261 and Alaα314) would not favour tyrosine binding in this place. A space-filling model of the PheRS–Tyr-AMP complex also shows no free space for an additional OH group of tyrosine. Thus, aromatic–aromatic interactions and van der Waals contacts discriminate between the nearly isosteric substrates, achieving highly specific recognition of the phenylalanine.

3.5. The metal-ion binding at the heterodimeric interface

The tightly bound divalent cation was first noted for magnesium in an apoenzyme structure (Mosyak *et al.*, 1995). The manganese has a relatively low *B* factor (31.3 $Å^2$) and is located within the tunnel of the heterodimeric interface formed by a number of polar residues from both α- and β-subunits, (Fig. 8). The manganese ion is coordinated by six electrostatic interactions with side chains of Aspβ452, Aspβ458, Gluβ461, Gluβ462 and Asnβ163 emerging from the β-subunit, and Gluα262 from the α-subunit. The latter residue belongs to the amino-acid-binding loop of the protein active centre. The position of the metal ion at the α/β-subunit interface, near the active site, obviously emphasizes its crucial role in PheRS structure and function: it is required for strengthening the heterodimer association and coordinating intersubunit electrostatic interactions; it also anchors the amino-acid-binding loop 255–263 containing the important Pheα258 and Pheα260.

3.6. Sulfate ion at the surface of proposed DNA-binding domain

The two residues Argβ407 and Argβ413 involved in the sulfate ion binding belong to helix H10 of the B5 domain (residues 407–473). The architecture of this domain was found (Mosyak *et al.*, 1995) to be similar to that of the catabolite gene activator domain responsible for DNA binding (Schultz *et al.*, 1991) by means of a helix–turn–helix motif (HTH). Detailed comparison between the structures of the *E. coli* biotin synthetase/repressor protein (BirA) and *T. thermophilus* PheRS revealed that all three domains of BirA, including the DNA-binding domain, appeared to have counterparts in the structure of PheRS (Safro & Mosyak, 1995). Structural relationships between the DNA-binding domain of BirA and the B5 domain of PheRS β-subunit made it possible to draw an analogy with the BirA repressor function and enabled us to hypothesize that PheRS is also involved in cell-regulatory processes *via* specific interaction with DNA molecules. Recently, biochemical experiments (Dou *et al.*, 2001; Ivanov *et al.*, 2000) on the DNA-binding activity of *T. thermophilus* PheRS provided evidence in favour of this hypothesis.

It is notable from the multiple sequence alignment, which includes both prokaryotic and eukaryotic PheRSs isolated from different species, that the portion of the sequence associated with the proposed DNA-binding domain (B5) is among the most conserved (Rodova *et al.*, 1999).

The highly ordered negatively charged divalent ion can be considered as an integral part of the DNA–PheRS interface and may play a crucial role in the recognition process, keeping side chains of the two arginines in positions ready to interact with the nucleic acid. Alternatively, this ion may be displaced from its position by negatively charged atoms of DNA and/or

replaced by a water molecule that mediates contacts to the protein in the complex.

3.7. Implication of structural aspects for the aminoacylation mechanism

Analysis of three-dimensional structures of PheRS complexed with functional ligands (PheRS–tRNA^{Phe}, PheRS–Phe and PheRS–Phe-AMP) and sequences of PheRS from several species together with biochemical data allow us to propose structural guidelines for phenylalanine substrate activation and conformational rearrangement of the 3′-terminal portion of cognate tRNA^{Phe} in the presence of adenylate. The location of the phenylalanine moiety observed in the PheRS–Phe-AMP complex and in the PheRS structure with phenylalanine alone (Reshetnikova *et al.*, 1999) shows that the free amino acid binds and maintains a position close to that in the phenylalanyl-adenylate. Furthermore, the class II conserved mode of ATP binding and the hydrogen-bonded distance of Argα204 from the α-phosphate of ATP and the carbonyl O atom of phenylalanine provide good evidence that the reactants are located in the active site of PheRS in accordance with an in-line mechanism for phenylalanine activation to occur.

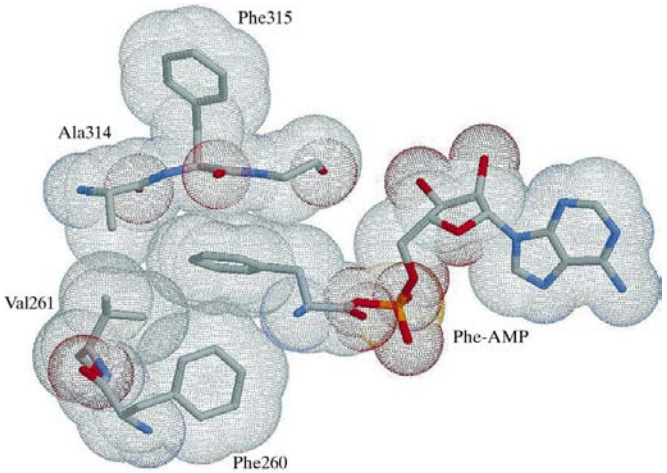

Figure 7
Sterical and hydrophobic constraints on phenylalanyl-adenylate binding. Space-filling representation of phenylalanyl-adenylate and protein residues that constitute the amino-acid binding cavity are shown as dots coloured to match the corresponding atoms in the stick models.

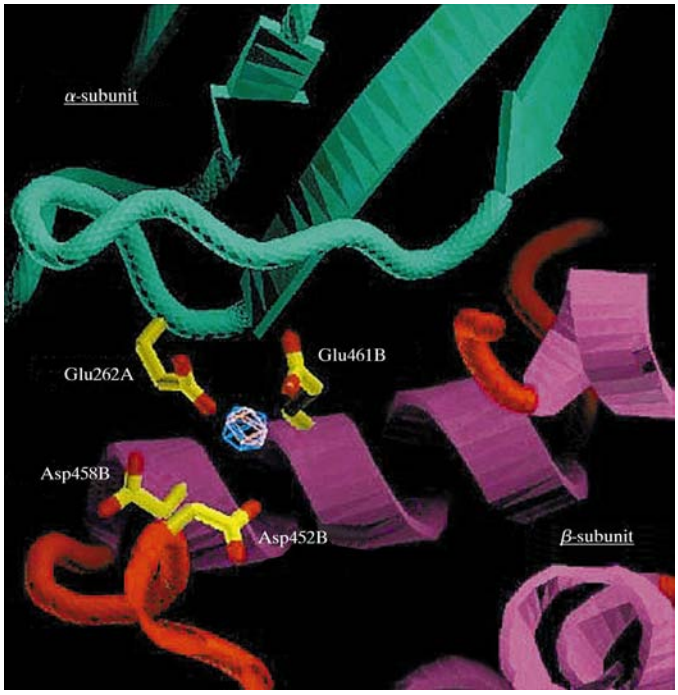

Figure 8
Manganese ion at the α/β interface. Electron-density peaks corresponding to an Mn^{2+} cation are shown in blue on a $2F_o - F_c$ map (contour level 7σ) and in red on anomalous map (contour level 5σ). The β-subunit is coloured red and magenta and the α-subunit cyan. Mn^{2+} is coordinated with four amino-acid residues: one from the α-subunit and three from the β-subunit. Asnα163 and Gluα461 are not shown for clarity.

In accordance with the mechanism of amino-acid activation described for class II aaRSs (Arnez & Moras, 1997), the geometry and charge of a pentacovalent transition state should be stabilized by positively charged amino acids and a divalent cation (magnesium or manganese). The role of the divalent cation in stabilizing the ATP conformation and adenylate formation is exemplified by Mg^{2+} ions revealed in the structures of SerRS (Belrhali *et al.*, 1995), AspRS (Cavarelli *et al.*, 1994), GlyRS (Arnez *et al.*, 1999) and AsnRS (Berthet-Colominas *et al.*, 1998) complexes with ATP, adenylate or adenylate analogues. However, in the histidine system, the divalent cation is replaced by HisRS-specific Arg259, which directly interacts with the adenylate phosphate on the side opposite to the guanidinium group of the class II conserved Arg113. These two arginines increase the electrophilicity of the α-phosphate group of ATP and lead to nucleophilic attack by the carboxylic group of the amino acid on the α-phosphate of ATP, followed by expulsion of PP_i.

In the phenylalanine system, the negative charge of the carbonyl O atom in the transition state is stabilized by three positively charged polar residues located within hydrogen-bonding distance, Argα204, Hisα178 and Glnα218, as well as by Trpα149. Trpα149 appears to be disordered, lacking electron density in PheRS complexed with the phenylalaninyl-adenylate, where the carbonyl group is substituted by the methylene group (Reshetnikova *et al.*, 1999). In the complex with the true aminoacyl-adenylate this residue is well ordered and clearly visible in the map. When superposing these two complexes, the largest conformational shift of $\sim$1.6 Å is observed for the polypeptide segment 138–151 comprising Trpα149. In the PheRS–Phe-AMP structure this segment is displaced towards the substrate, thus providing hydrogen-bond formation between the N atom of the indole ring and the carbonyl O atom of the adenylate.

There is no electron density in the anomalous Fourier difference map which can be unambiguously identified as anomalous scatterers, *i.e.* manganese ions in the active site of the PheRS–Phe-AMP complex (apart from the manganese at the interface area). Thus, currently available experimental evidence suggests two possibilities: (*a*) the formation of the stable intermediate Phe-AMP in the phenylalanine system may occur without divalent cation(s) or (*b*) these ions are

released after Phe-AMP formation. The detection of a manganese ion in the interface area ensures that the absence of the anomalous signal in the active site is not accidental and is an intrinsic characteristic of the phenylalanine system. We propose that the role of Mg^{2+} (which acts as an electrophilic catalyst) in the phenylalanine system is shared by two partners: the polar NH group of Trpα149 and the water molecule S290. Trp149 is not conserved in the other PheRS amino-acid sequences, but His and Gln at this position in other PheRSs (both in prokaryotes and eukaryotes) (Rodova *et al.*, 1999), are capable of participating in such an interaction. It is unlikely that the observed water molecule S290 is occupying the position of a 'principal magnesium ion' (Belrhali *et al.*, 1995) as there are no obvious candidates among the amino acids with polar side chains capable of participating in octahedral coordination of an Mg^{2+} ion, as happens in SerRS, AspRS, GlyRS and AsnRS. In fact, Glyα282 (in place of serine in SerRS) and Gluα279 (involved in solvent-mediated interactions with Argα252; see §3.3) occur in PheRS at positions suitable for electrostatic interaction in other class II aaRSs with a 'principal ion' (bridging the α- and β-phosphates of ATP) Mg^{2+} (or Mn^{2+}). It is possible to hypothesize that if ATP coupled with the metal ions triggers conformational changes disrupting the cluster of polar residues (Argα252, Glnα254, Glnα266 and Gluα279) linked to the water molecule S195, then the side chains of Gluα279 and Glnα266, being re-oriented towards the substrate, will come into play in the octacoordination of the divalent ion. Additional structural information on the PheRS-ATP + Mg^{2+} (or Mn^{2+}) complex is required to shed light on this problem.

The necessity for rearrangement of the tRNA terminal adenosine is evident from comparison of the structures of PheRS complexed with cognate $tRNA^{Phe}$ (Goldgur *et al.*, 1997) and Phe-AMP. In the structure of the PheRS-$tRNA^{Phe}$ complex, the position of the terminal adenosine Ade76 partially interferes with the position occupied by phenylalanine in the complexes with Phe-AMP and Phe alone (Reshetnikova *et al.*, 1999). It is common for aaRSs, with a few exceptions (GlnRS, GluRS and ArgRS), that the formation of aminoacyl-adenylate, the first intermediate of the aminoacylation reaction, does not require the presence of tRNA molecules. Moreover, adenylate formation is a prerequisite for effective tRNA binding, as is known for some other class II synthetases: SerRS (Belrhali *et al.*, 1994) and AspRS (Cavarelli *et al.*, 1994). Thus, the 3′ end of the $tRNA^{Phe}$ should be correctly positioned in the presence of phenylalanyl-adenylate before the second stage of the aminoacylation reaction can proceed or, to put it differently, the presence of the intermediate may favour correct binding of the terminal adenosine of $tRNA^{Phe}$. Recent data on the affinity cross-linking of *T. thermophilus* PheRS with reactive $tRNA^{Phe}$ derivatives give another indication of the acceptor-end rearrangement in the presence of all the substrates (Vasil'eva *et al.*, 2000).

The position of the terminal adenosine in the active site, as shown in the PheRS-$tRNA^{Phe}$ complex (Goldgur *et al.*, 1997) is stabilized by three hydrogen bonds. N6 of Ade76 makes contacts with Serα180 and Gluα220; the indole ring of Trpα149 (which is approximately perpendicular to the base of Ade76) makes a hydrogen bond between $N^{\varepsilon 1}$ and N7 of the adenosine. As indicated above, in the PheRS–Phe-AMP complex the side chain of Gluα220 swings away significantly from its position in the PheRS–tRNA complex, making only indirect contact with the amino group of the substrate. Trpα149 is shifted out from its position towards the hydrogen-bonding position with the carbonyl O atom of the intermediate. The phenyl rings of both Pheα258 and Pheα260 also change their orientation. In this new environment, only Serα180 keeps the orientation shown in the PheRS–$tRNA^{Phe}$ complex.

The proposed mode of simultaneous positioning of Phe-AMP and the 3′-end of $tRNA^{Phe}$ in the active site of the protein is shown schematically in Fig. 9. Compared with its position in the tRNA complex, Ade76 may occupy a new position approaching adenylate from the 2′-OH group of its ribose moiety. This conformational rearrangement may be considered as an 'aromatic–aromatic exchange'. Penetrating into the amino-acid binding pocket in the PheRS–$tRNA^{Phe}$ complex, Ade76 forms an aromatic 'network' with Pheα258 and Pheα260, whereas in the presence of Phe-AMP it participates in formation of a 'network' with Pheα258 and Trpα149. Thus, phenylalanine from Phe-AMP and its neighbouring Pheα258 and Pheα260 create one aromatic triad, while Ade76 and Pheα258 together with Trpα149 create another triad. These two adjacent aromatic–aromatic triads in turn may create a six-member 'network' which is highly preferable in terms of potential energy and thus stabilizes the ternary PheRS–Phe-AMP–$tRNA^{Phe}$ complex within the active site and orients its reactants ready for the second step of aminoacylation to proceed. The aromatic–aromatic interaction between Ade76 and Trp149 may be substituted by

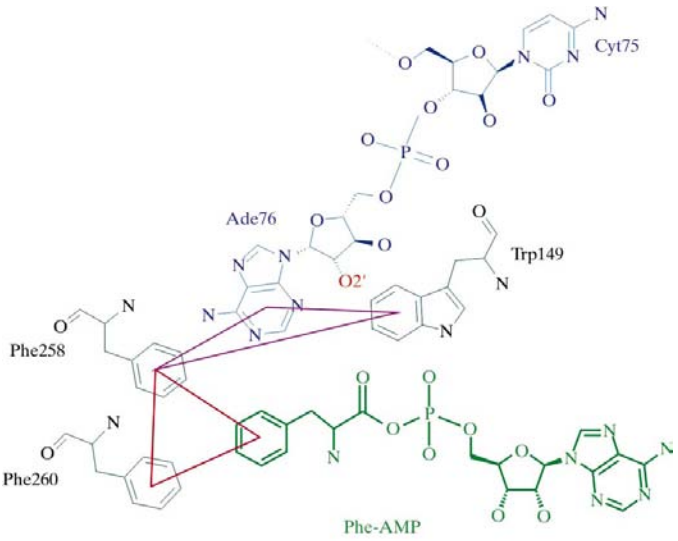

Figure 9
The schematic diagram for proposed mode of interactions at the active site for a ternary complex PheRS (black) with Phe-AMP (green) and $tRNA^{Phe}$ (blue). Two triple 'edge-to-face' aromatic interactions at the active site are indicated with red and magenta triangles. The 2′-OH group of the ribose of the tRNA terminal Ade76 is shown in red.

hydrogen bonding between N7 of adenosine and side chains of Gln or His, which may replace Trp149 at this position in other PheRSs.

In the second step of $tRNA^{Phe}$ aminoacylation, the 2′-OH of the terminal Ade76 ribose attacks the carbonyl C atom of the Phe-AMP intermediate. The NH group of Trpα149 is suitably located to catalyze the attack of the ribose 2′-OH of the Ade76 on the carbonyl O atom of Phe-AMP. An in-depth analysis of the stereochemical parameters of the aminoacylation reaction could be provided by a three-dimensional structure of the ternary complex between PheRS–$tRNA^{Phe}$ and the non-hydrolysable Phe-AMP analogue.

We are grateful to the staff of the X12C beamline of Brookhaven NSLS for their help during data collection. We thank Professor W. Traub for reading and correction of the manuscript. This work was supported by Kimmelman Center for Biomolecular Structure and Assemblies and INTAS grant (No. 97-2110).

References

Åberg, A., Yaremchuk, A., Tukalo, M., Rasmussen, B. & Cusack, S. (1997). *Biochemistry*, **36**, 3084–3094.
Ankilova, V., Reshetnikova, L., Chernaya, M. & Lavrik, O. (1988). *FEBS Lett.* **227**, 9–13.
Arnez, J. G., Augustine, J. G., Moras, D. & Franklyn, C. S. (1997). *Proc. Natl Acad. Sci. USA*, **94**, 7144–7149.
Arnez, J., Dock-Bregeon, A.-C. & Moras, D. (1999). *J. Mol. Biol.* **286**, 1449–1459.
Arnez, J., Harris, D., Mitschler, A., Rees, B., Francklyn, C. & Moras, D. (1995). *EMBO J.* **14**, 4143–4155.
Arnez, J. & Moras, D. (1997). *Trends Biochem. Sci.* **22**, 211–216.
Belrhali, H., Yaremchuk, A., Tukalo, M., Berthet-Colominas, C., Rasmussen, B., Bösecke, P., Diat, O. & Cusack, S. (1995). *Structure*, **3**, 341–352.
Belrhali, H., Yaremchuk, A., Tukalo, M., Larsen, K., Berthet-Colominas, C., Leberman, R., Beijer, B., Sproat, B., Als-Nielsen, J., Grübel, G., Legrand, J.-F., Lehmann, M. & Cusack, S. (1994). *Science*, **263**, 1432–1436.
Berthet-Colominas, C., Seignovert, L., Härtlein, M., Groti, M., Cusack, S. & Leberman, R. (1998). *EMBO J.* **17**, 2947–2960.
Biou, V., Yaremchuk, A., Tukalo, M. & Cusack, S. (1994). *Science*, **263**, 1404–1410.
Bobkova, V. E., Volfson, A. D., Ankilova, V. N. & Lavrik, O. I. (1991). *FEBS Lett.* **290**, 95–98.
Brunger, A., Adams, P., Clore, G. M., DeLano, W., Gros, P., Grosse-Kunstleve, R., Jiang, J.-S., Kuszewski, J., Nilges, N., Pannu, N., Read, R., Rice, L., Simonson, T. & Warren, G. (1998). *Acta Cryst.* D**54**, 905–921.
Burley, S. & Petsko, G. (1985). *Science*, **229**, 23–28.
Carson, M. (1997). *Methods Enzymol.* **277**, 493–505.
Cavarelli, J., Eriani, G., Rees, B., Ruff, M., Boeglin, M., Mitschler, A., Martin, F., Gangloff, J., Thierry, J. C. & Moras, D. (1994). *EMBO J.* **13**, 327–337.
Chernaya, M., Korolev, S., Reshetnikova, L. & Safro, M. (1987). *J. Mol. Biol.* **198**, 555–556.
Collaborative Computational Project, Number 4 (1994). *Acta Cryst.* D**50**, 760–763.
Cusack, S. (1995). *Nature Struct. Biol.* **2**, 824–831.
Cusack, S., Berthet-Colominas, C., Härtlein, M., Nassar, N. & Leberman, R. (1990). *Nature (London)*, **347**, 249–255.
Cusack, S., Yaremchuk, A., Krikliviy, I. & Tukalo, M. (1998). *Structure*, **6**, 101–108.
Cusack, S., Yaremchuk, A. & Tukalo, M. (1996). *EMBO J.* **15**, 6321–6334.
Delarue, M., Poterszman, A., Nikonov, S., Garber, M., Moras, D. & Thierry, J. C. (1994). *Curr. Opin. Struct. Biol.* **5**, 48–55.
Desogus, G., Todone, F., Brick, P. & Onesti, S. (2000). *Biochemistry*, **39**, 8418–8425.
Dou, X., Limmer, S. & Kreutzer, R. (2001). *J. Mol. Biol.* **305**, 451–458.
Eriani, G., Delarue, M., Poch, O. & Moras, D. (1990). *Nature (London)*, **347**, 203–206.
Goldgur, Y., Mosyak, L., Reshetnikova, L., Ankilova, V., Lavrik, O., Khodyreva, S. & Safro, M. (1997). *Structure*, **15**, 59–68.
Ivanov, K., Moor, N., Ankilova, V. & Lavrik, O. (2000). *Biochemistry (Moscow)*, **65**, 436–441.
Jones, T., Zou, J.-Y., Cowan, S. W. & Kjeldgaard, M. (1991). *Acta Cryst.* A**47**, 110–119.
Khodyreva, S., Moor, N., Ankilova, V. & Lavrik, O. (1985). *Biochem. Biophys. Acta*, **830**, 206–212.
Laskowski, R. A., MacArthur, M. W., Moss, D. S. & Thornton, J. M. (1993). *J. Appl. Cryst.* **26**, 283–291.
Logan, D. T., Mazauric, M.-H., Kern, D. & Moras, D. (1995). *EMBO J.* **14**, 4156–4167.
Mosyak, L., Reshetnikova L., Goldgur Y., Delarue, M. & Safro, M. (1995). *Nature Struct. Biol.* **2**, 537–547.
Nicholls, A., Sharp, K. A. & Honig, B. (1991). *Proteins*, **11**, 281–286.
Onesti, S., Miller, A. D. & Brick, P. (1995). *Structure*, **3**, 163–176.
Otwinowski, Z. (1993). *Proceedings of the CCP4 Study Weekend. Data Collection and Processing*, edited by L. Sawyer, N. Isaacs & S. Bailey, pp. 56–62. Warrington: Daresbury Laboratory.
Pepinsky, R. & Okaya, Y. (1956). *Proc. Natl Acad. Sci. USA*, **42**, 286–292.
Poterszman, A., Delarue, M., Thierry, J.-C. & Moras, D. (1994). *J. Mol. Biol.* **244**, 158–167.
Read, R. (1986). *Acta Cryst.* A**42**, 140–149.
Reshetnikova, L., Moor, N., Lavrik, O. & Vassylyev, D. (1999). *J. Mol. Biol.* **287**, 555–568.
Richardson, J. (1981). *Adv. Protein Chem.* **34**, 167.
Rodova, M., Ankilova, V. & Safro, M. (1999). *Biochem. Biophys. Res. Commun.* **255**, 765–772.
Ruff, M., Krishnaswamy, A., Boeglin, M., Poterszman, A., Mitschler, A., Podjarny, A., Rees, B., Thierry, J. C. & Moras, D. (1991). *Science*, **252**, 1682–1689.
Safro, M. & Mosyak, L. (1995). *Protein Sci.* **4**, 2429–2432.
Sankaranarayanan, R., Dock-Bregeon A. C., Romby, P., Caillet, J., Springer, M., Rees, B., Ehresmann, C., Ehresmann, B. & Moras, D. (1999). *Cell*, **97**, 371–381.
Schmitt, E., Moulinier, L., Fujiwara, S., Imanaka, T., Thierry, J.-C. & Moras, D. (1998). *EMBO J.* **17**, 5227–5237.
Schultz, S., Shields, G. & Steitz, T. (1991). *Science*, **253**, 1001–1007.
Vasil'eva, I. A., Ankilova, V. N., Lavrik, O. I. & Moor, N. A. (2000). *Biochemistry (Moscow)*, **60**, 1157–1166.
Yamane, T. & Hopfield, J. J. (1977). *Proc. Natl Acad. Sci. USA*, **74**, 2246–2250.